Scaling of the Rotational Relaxation of Tracers in *o*-Terphenyl: A Linear and Nonlinear ESR Study

L. Andreozzi,* M. Faetti, M. Giordano, and D. Leporini

Dipartimento di Fisica, Università di Pisa, Piazza Torricelli 2, I-56126 Pisa, Italy, and INFM, UdR Pisa, I-56126 Pisa, Italy

Received: September 29, 1998; In Final Form: March 9, 1999

The rotational dynamics at long and short times of nearly spherical and cylindrical tracers in supercooled and glassy *o*-terphenyl is investigated by linear and nonlinear electron spin resonance spectroscopy, respectively. The short-time and long-time dynamics are characterized by the effective correlation times τ_s and τ_l, respectively. At higher temperatures, the relaxation is exponential and the Debye−Stokes−Einstein law (DSE) holds, $\tau_s \approx \tau_l \propto \eta$. η is the shear viscosity. On cooling, the rotational dynamics is partially coupled to the viscosity. At lower temperatures the reorientation is activated. Interestingly, on the short time scale the rotational correlation times of the two tracers (τ_s) in a wide temperature range down to the activated regime collapse in a single curve by proper scaling. The scaling does not work at long times (τ_l).

1. Introduction

The diffusion in liquids is usually described in the framework of Brownian motion which leads to the Stokes−Einstein (SE)[1] and the Debye−Stokes−Einstein (DSE) laws.[2] The former relates to the translation, the latter to the reorientation. They state that the inverse of the diffusion coefficient D^{-1} and the rotational correlation time of the tagged particle τ are proportional to the shear viscosity η. In particular, DSE predicts for a sphere of volume V:

$$\tau = \frac{V\eta}{k_B T} \tag{1}$$

k_B is the *Boltzmann* constant; T is the temperature. No-slip (stick) boundary conditions are assumed by eq 1, which has been generalized to ellipsoids with different boundary conditions.[3]

Both SE and DSE rest on the hydrodynamics and the Langevin formulation of the Brownian motion.[1] In particular, the liquid is treated as structureless and with vanishing response time so that the friction experienced by the particle at the time t depends on the velocity of the particle at the same time. These assumptions imply that *both* the space and time scales of the liquid are shorter than the corresponding ones of the tagged molecule. On this basis, the breakdown of DSE and SE is expected if scales of the tagged molecule and the host liquid become comparable.

Despite the severe assumptions leading to SE and DSE, their robustness is remarkable, which has been extensively verified even in the molecular self-diffusion of low-viscosity liquids. The results suggest that a failure of SE and DSE implies that the relevant space and the time scales of the tagged molecules must be fairly shorter than the ones of the host. Materials where that regime is highly expected are the supercooled liquids and polymers. In fact, diffusion coefficients and rotational relaxation rates exceeding the predictions of SE and DSE in supercooled molecular liquids[4−9] and polymers[10−14] are reported. Similar effects are also known for dc conductivity of ionic melts.[15] Key features of these materials are the nonexponential slow relaxation rate and the repeated evidence from experiments[16,17] and numerical work[18,19] of so-called "dynamical heterogeneities", namely parts of the sample being characterized by different dynamical properties. For a review on this topic see ref 20. The role of the heterogeneities in the breakdown of SE and DSE is anticipated[6−8,14,21−23] and has received much attention in both theoretical[23] and numerical studies.[24−26]

The present work presents new experimental efforts aimed at gaining further insight concerning the reorientation in supercooled liquids. In particular, the rotational dynamics of stiff, molecular tracers with different symmetries in supercooled and glassy *o*-terphenyl (OTP) is studied both on the long-time scale by linear ESR spectroscopy (up to 10^{-7} s) and on the short-time scale by the LODESR spectroscopy (about 10^{-10} s).

The interest is turned to the decoupling of the tracer rotation from the viscosity. It is shown that, irrespective of the tracer, on both long-time and short-time scales, the temperature dependence of the correlation times exhibits three, clearly defined regimes. At higher temperatures DSE (eq 1) holds. At intermediate temperatures a crossover regime is observed. At lower temperatures the reorientation is activated. The crossover temperatures between the three regimes and the parameters of DSE and Arrhenius laws characterizing them are found to depend on the tracers. Nonetheless, quite interestingly, the data on the short-time scale of the two tracers are collapsed on a single curve by proper scaling. The scaling does not work on the long-time scale.

2. Background on the Linear and Nonlinear ESR

The electron spin resonance (ESR) spectroscopies are powerful tools to investigate the rotational dynamics in liquids and polymers.[27−29] The study is carried out by dissolving suitable paramagnetic molecules (spin probes). In particular, nitroxide spin probes, with electronic spin $S = {}^1/_2$ and nuclear spin $I = 1$, are of current use due to both thermal stability and their well-characterized magnetic interactions and ESR spectrum.[28]

In linear X-band ESR experiments, the spin system, acted on by a static magnetic field H_0, is irradiated by a microwave field ($\nu \cong 10^{10}$ Hz), inducing the σ transition between the

* E-mail: andreozz@difi.unipi.it.

10.1021/jp983896r CCC: $18.00
Published on Web 04/13/1999

Zeeman levels. The transverse component of the magnetization M with respect to H_0 is detected. In the linear response regime the line shape is independent of the microwave field, whereas it is deeply affected by the tracer rotations. In fact, the reorientation of the spin probe results in random time dependent magnetic fields, originating from the anisotropic character of the magnetic interactions, which drives the magnetization to the equilibrium.[27−29] In particular, the transverse magnetization relaxes via a phase-loss mechanism.

In the case of the X-band linear ESR spectroscopy, the investigated correlation times range between 10^{-12} s $\leq \tau \leq 10^{-7}$ s. They are drawn by proper algorithms accounting for the stochastic nature of the molecular motion.[29−31]

In the present study, the rotational dynamics of the tracers in OTP has been modeled by considering rotational diffusion[32,33] and jump diffusion[34,35] models. The adjustable parameters of the diffusion model are the eigenvalues of the diffusion tensor, $D_{\|}$ and $D_{\perp}$ in the case of tracer with cylindrical symmetry. The former refers to rotations around the symmetry axis, the latter to rotations of the symmetry axis. The adjustable parameters of the jump model are the residence time τ_0, i.e., the average time spent before the jump occurs, and the jump angle ϕ. To compare the two models, we define $\tau = \tau_0/[1 - \sin(5\phi/2)/(5 \sin \phi/2)]$, $\tau_{\|} = {}^1/_6 D_{\|}$ and $\tau_{\perp} = {}^1/_6 D_{\perp}$. For spherical molecules reorientating by small jump angles, $\tau = \tau_{\|} = \tau_{\perp} = \tau_0/\phi^2$. If the jumps are large, τ is the area below the correlation function of the spherical harmonic $Y_{2,0}$.[34,35]

The longitudinally detected electron spin resonance spectroscopy (LODESR), developed in this laboratory[29,36] irradiates the spin system, in resonance conditions, by two σ-polarized microwaves with angular frequencies ω_1 and ω_2, which are close to the Larmor frequency $\omega_0 = \gamma H_0$, γ being the gyromagnetic factor. Differently from ESR, the parallel component of the magnetization M with respect to H_0, M_z, is detected.

The process observed by LODESR is the absorption of a photon at ω_1 (ω_2) followed by the emission of a photon at ω_2 (ω_1). According to the conservation of the angular momentum, it is referred to as a longitudinal process since M_z is affected.[29,36,37] The nonlinear response of the spin system to the two microwave fields manifests in the presence of harmonics oscillating at $m|\omega_2 - \omega_1|$, $m = 1, 2, \ldots$. It must be noted that the nonlinear nature of LODESR is due to the multiple irradiation and not the amplitudes of the microwave fields, which are small.

In the case of the X-band LODESR spectroscopy, the investigated correlation times range between 10^{-12} s $\leq \tau \leq 10^{-5}$ s. The full interpretation of the signal implies the definition of two different dynamical regimes, the slow-fluctuation regime ($\tau > \omega_0^{-1}$) and the fast-fluctuation regime.

It has been proved under fairly general conditions that the relaxation of the longitudinal magnetization M_z in the slow-fluctuation regime $\tau > \omega_0^{-1}$ relaxes exponentially with decay time given by the longitudinal relaxation time T_1.[37,38] T_1 depends on the energy exchanges between the spin system and the thermal bath embedding the spin system itself and provides additional new information with respect to the relaxation of the transverse magnetization detected by ESR.[30]

The T_1 value for dilute solutions of nitroxide spin probes is due to the anisotropy of the Zeeman and hyperfine magnetic interactions and the spin−rotation interaction:[39]

$$\frac{1}{T_1} = \left(\frac{1}{T_1}\right)_{\mathrm{Z,H}} + \left(\frac{1}{T_1}\right)_{\mathrm{SR}} \tag{2}$$

The contribution due to the Zeeman and hyperfine magnetic interactions is[39,40]

$$\left(\frac{1}{T_1}\right)_{\mathrm{Z,H}} = \frac{2}{5\omega_0^{\,2}\tau_{s\perp}}\left[\frac{1}{2}(F_{\mathbf{g}}^{(2,0)})^2 + \frac{10}{9}(F_{\mathbf{A}}^{(2,0)})^2 + \frac{1}{3}(F_{\mathbf{g}}^{(2,2)})^2 + \frac{20}{27}(F_{\mathbf{A}}^{(2,2)})^2\right] + \frac{2}{5\omega_0^{\,2}\tau_{s\|}}\left[\frac{2}{3}(F_{\mathbf{g}}^{(2,2)})^2 + \frac{40}{27}(F_{\mathbf{A}}^{(2,2)})^2\right] \tag{3}$$

$F^{(2,m)}$, $m = 0, 2$, are particular spherical components of the tensors $\mathbf{g}\beta H_0$ (Zeeman) and $\mathbf{A}$ (hyperfine), β being the Bohr magneton.[27−29] In terms of their Cartesian components of the tensors $F^{(2,0)} = [2F_{zz} - (F_{xx} + F_{yy})]/\sqrt{6}$ and $F^{(2,\pm 2)} = [F_{xx} - F_{yy} \pm i(F_{xy} + F_{yx})]/2$. In eq 4 the tensors are expressed in their molecular principal frame where $F_{ij} = 0$ if $i \neq j$.

The term due to the spin−rotation interaction is[39,40]

$$\left(\frac{1}{T_1}\right)_{\mathrm{SR}} = \frac{2}{27}[(\delta g_x)^2 + (\delta g_y)^2]\left[\frac{1}{\tau_{s\perp}} + \left(\frac{I_{\|}}{I_{\perp}}\right)^2 \frac{1}{2\tau_{s\|}}\right] + \frac{2}{27}(\delta g_z)^2\left[\frac{1}{2\tau_{s\|}} + \left(\frac{I_{\perp}}{I_{\|}}\right)^2 \frac{1}{\tau_{s\perp}}\right] \tag{4}$$

$\delta g_i = g_i - g_e$ with $g_e = 2.0023$. $I_{\|}$ and $I_{\perp}$ are the principal values of the moments of inertia of the spin probe.

In the fast-fluctuation regime $\tau < \omega_0^{-1}$, derivations of the LODESR line shape are reported.[39] The experimental procedure to draw the correlation times from the line shape includes a careful evaluation of the contributions of intermolecular interactions, dipolar and exchange, which assume particular importance at higher temperatures. Detailed discussion is found elsewere.[39]

Due to the sensitivity of linear and nonlinear ESR spectroscopies to adiabatic and nonadiabatic relaxation, respectively, they are able to provide selective information on the power spectrum $J(\omega)$ of the rotational correlation functions.

In liquids with medium and high viscosity, linear ESR spectroscopy turns out to be mainly sensitive to component $J(0)$, and therefore linear ESR selects the *long* time scales of the decay of the correlation function. To emphasize the point, the correlation times drawn by ESR will be referred to by the label "*l*", e.g., $\tau_{l\|}$. If a distribution of correlation times is expected, it is understood that τ_l must be read as $\langle\tau_l\rangle$, where the brackets denotes the average over the distribution. Differently, the relaxation of the longitudinal magnetization is mainly driven by the component of the power spectrum at the Larmor frequency $J(\omega_0)$, making the LODESR spectroscopy sensitive to the short-time (of the order of $1/\omega_0$) decay of the rotational correlation function.[12,13,27−31,36−39] The correlation times drawn by LODESR are referred to by the label "s". In the slow-fluctuation regime ($\omega_0\tau_s > 1$) in the presence of a distribution of correlation times, $1/\tau_s$ must be read as $\langle 1/\tau_s\rangle$.[40]

In the presence of non exponential relaxation, the ESR and LODESR spectroscopies provide distinct values for the correlation times, τ_l and τ_s, respectively, the latter being shorter than the former.[12,13] The equality $\tau_l = \tau_s$ is a signature of the exponential decay of the rotational correlation functions.

3. Experimental Section

OTP (99% Aldrich, $T_g = 243$ K) is a well-known fragile glass former. The molecular structure is shown in Figure 1. The approximate van der Waals radius is $r_{OTP} = 3.7$ Å.[8] The tracers (nitroxide spin probes) dissolved in OTP are TEMPO and CHOLESTANE (Aldrich) which were used as-received (Figure 1). Both of them are stiff molecules. The TEMPO molecule is nearly spherical in shape, while CHOLESTANE can be approximated by a cylinder.[28] 3D models of OTP and the tracers

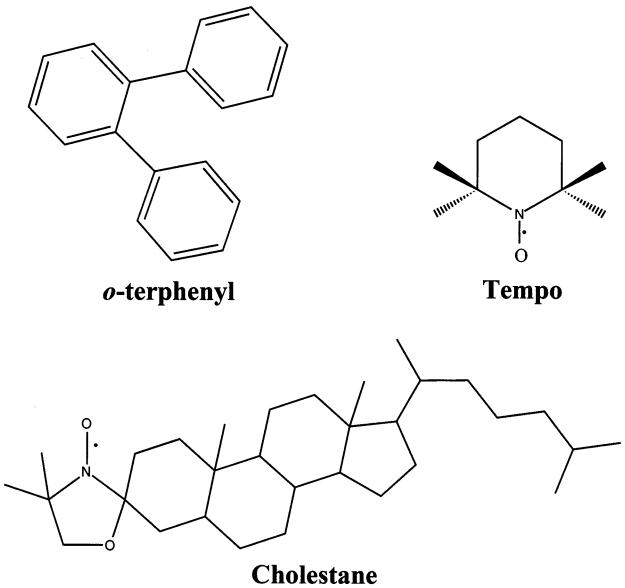

Figure 1. Chemical structure of OTP, TEMPO, and CHOLESTANE molecules.

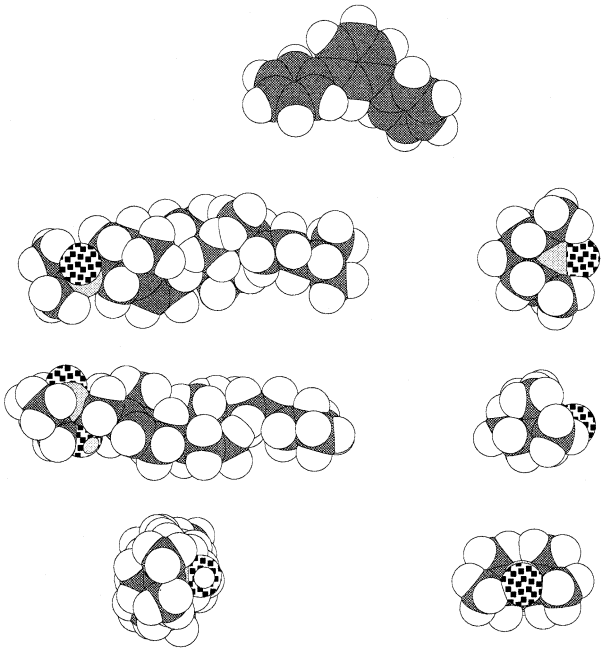

Figure 2. 3D models of OTP (top) and the side, top, and front views of CHOLESTANE (left) and TEMPO (right). TEMPO is nearly spherical whereas CHOLESTANE is rodlike.

have been developed by Chem3D (Figure 2). TEMPO may be sketched as an oblate ellipsoid (disklike) with semiaxis $a_{||} \approx 2.7$ Å, $a_{\perp} \approx 3.7$ Å. The radius of the equivalent sphere $r_{\mathrm{TEMPO}} \approx 3.4$ Å, is comparable with the van der Waals radius of OTP. CHOLESTANE is similar to a prolate ellipsoid (rodlike) with semiaxis $a_{||} \approx 9.9$ Å and $a_{\perp} \approx 2.9$ Å. The inertia moments of CHOLESTANE, as evaluated by the 3D model, leads to the anisotropy ratio $(I_{\perp}/I_{||})_{\mathrm{th}} = 12.4$, which is comparable to the experimental one $(I_{\perp}/I_{||})_{\mathrm{ex}} = 17$ obtained by measuring the line widths of the linear ESR signal of diluted solutions (2×10^{-4} mol/L) of CHOLESTANE in OTP.[39] The N−O bond where the unpaired spin is located lies in the plane normal to the symmetry axis of both TEMPO and CHOLESTANE. Magnetic parameters of both spin probes in OTP were drawn by careful analysis of the ESR powder spectrum recorded at 166 K.[28−30]

TEMPO and CHOLESTANE were dissolved in OTP in

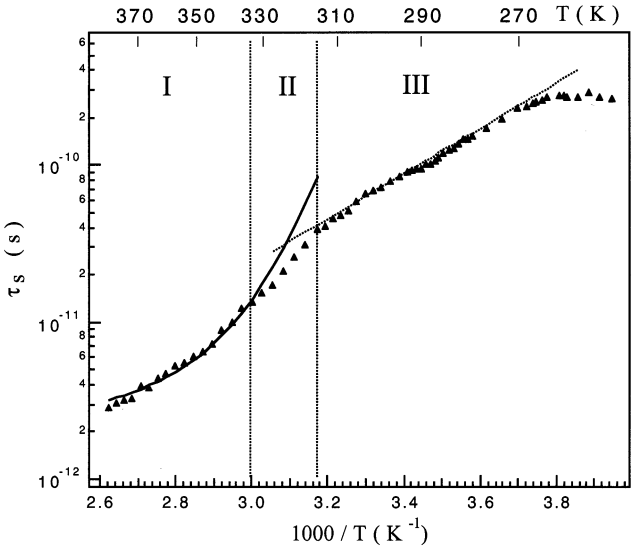

Figure 3. Temperature dependence of the short-time correlation time τ_s for TEMPO in OTP. Continuous line: fit with DSE (eq 1). Dotted line: fit with Arrhenius law. The activation energy and the attempt rate are 27.1 ± 0.7 kJ/mol and 7.8×10^{13} s^{-1}, respectively.

concentration 10^{-3} and 8×10^{-3} mol/L for studies of linear ESR and LODESR, respectively. As far as the higher concentration is concerned, the choice is the best compromise between the need to optimize the signal-to-noise ratio, LODESR being a second-order spectroscopy, and the need to minimize both the intermolecular magnetic interaction and the perturbation of the host by the tracer. The samples were degassed and sealed in an ultrapure N_2 (99.995%) atmosphere. For both concentrations, differential scanning calorimetry experiments have shown no plasticization effects in OTP due to the presence of the tracers. In agreement with previous studies,[7] decreasing the spin probe concentration did not result in any change of the correlation times. The tests rule out the hypothesis that the deviations from the DSE law can be ascribed to tracer effects and allow the use of the viscosity data of neat OTP.[41]

Mesurements of linear ESR spectroscopy were carried out by a Bruker ER200D spectrometer, equipped with microwave X-band bridge. LODESR measurements were carried out by a home-built X-band spectrometer. Details can be found elsewhere.[36]

4. Results and Discussion

The values of the correlation times τ_s of TEMPO are shown in Figure 3.[13] Three different dynamical regions are identified.

In region I ($T > T_{\mathrm{D-I}} \equiv 333$ K), which extends over about 50 K, τ_s is proportional to the viscosity and agrees with DSE, eq 1. At $T_{\mathrm{D-I}} \equiv 333$ K the decoupling from the viscosity is observed. In region II, extending over about 20 K, the temperature dependence of τ_s is weaker than the viscosity one. Figure 4 plots the data of region II vs η/T. In region III of Figure 3 ($T < T_{\mathrm{I-A}} \equiv 315$ K) an activated dynamical regime of τ_s is observed, which becomes weaker below $T_{\mathrm{A-A}} \equiv 270$ K. Note that the Arrhenius regime occurs at $T > T_g$ and suggests that, since the tracer reorientation is faster than the host dynamics, the reorientation at short time ($\tau_s \approx 2 \times 10^{-10}$ s) occurs in a frozen environment. The decrease of the activation energy at lower temperatures is understood by noting that the tracer is largely decoupled by the host dynamics and then it may rearrange itself by different, activated alternatives. The crossover

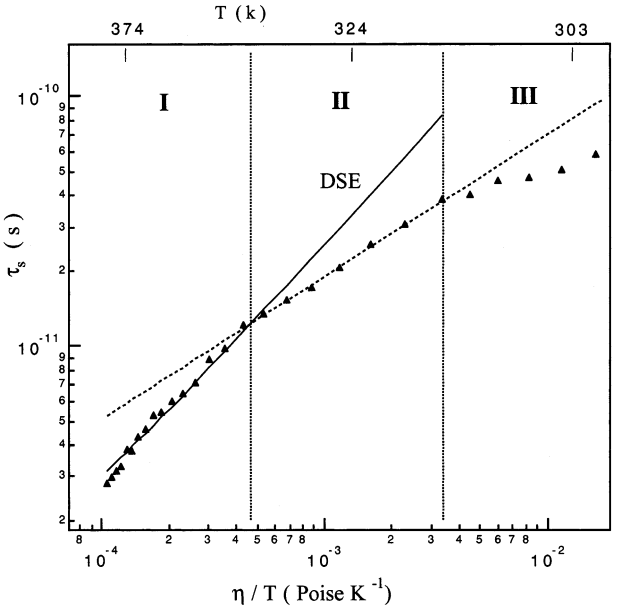

Figure 4. Region II of TEMPO in OTP as a function of η/T. The continuous line is the prediction by DSE (see also Figure 3). The dashed line is a guide for the eyes. Note the change of dynamical regime occurring at the boundaries of the region at 333 and 315 K.

TABLE 1: Short-Time Reorientation of the Tracers[a]

tracer	T_{D-I} (K)	T_{I-A} (K)	T_{A-A} (K)	ΔE_1 (kJ/mol)	ΔE_2 (kJ/mol)
TEMPO	333	315	270	27.1	4.2
CHOLESTANE	342	328	281	15.0	2.4

[a] Crossover temperatures between the DSE and intermediate regimes (T_{D-I}), the intermediate- and the high-temperature activated regime (T_{I-A}), and the high-temperature and the low-temperature activated regimes (T_{A-A}). The activation energies of the high-temperature (1) and the low-temperature (2) activated regimes are also listed.

temperatures between the dynamical regimes of the short-time reorientation of TEMPO and other relevant quantities are summarized in Table 1.

The comparison between the short-time (τ_s) and the long-time (τ_l) reorientation of TEMPO in OTP is presented in Figure 5.[13] It reveals that the long-time behavior exhibits three regions in close analogy with the short-time one, namely a high-temperature region where DSE holds, an intermediate regime, and an activated regime at lower temperatures. At higher temperatures the equality $\tau_s = \tau_l$ holds, showing that the correlation loss is exponential (see section 2) and that τ_l agrees with DSE.[7] By assuming slip boundary conditions,[3] fitting eq 1 to τ_l yields the TEMPO radius $r \cong 2.6$ Å to be compared with the average van der Waals radius $r_W = 3.4$ Å. The change of regime on the short-time scale at 333 K breaks the exponential behavior and signals the onset of new time scales. At 298 K the decoupling of τ_l and viscosity takes place. In the range 298 K $> T >$ 280 K, which includes the critical temperature of OTP predicted by the mode coupling theory of the glass transition[4,42] T_c =290 K, a crossover regime is observed. For $T <$ 270 K previous ESR studies showed that TEMPO rotates at long times by activated jumps in a frozen structure.[35] For $T > T_g$ an activation energy of 18.7 kJ/mol and an attempt rate 1.3 $\times 10^{12}$ s^{-1} are found; for $T < T_g$ 4.4 $\pm$ 0.4 kJ/mol and attempt rate 4.2 $\times 10^8$ s^{-1} are found. As a final remark on the TEMPO reorientation, we point out that the crossovers between the three dynamical regimes observed at both short time and long time occurs at lower temperatures at long times.

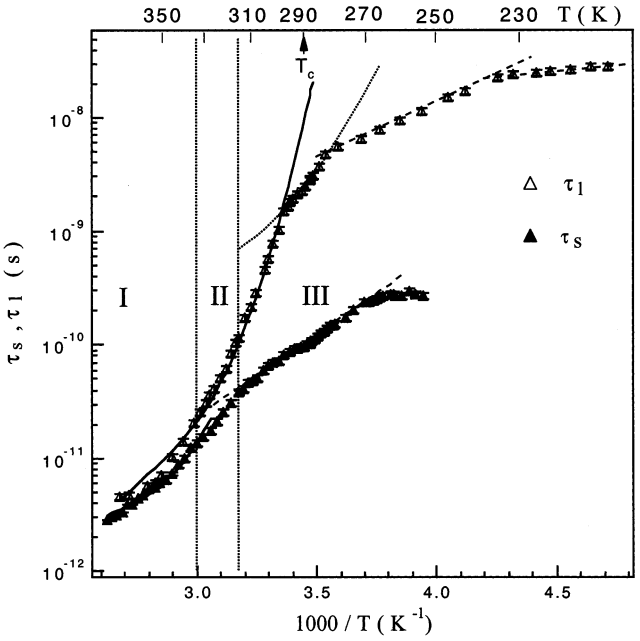

Figure 5. Comparison of the temperature dependence of the correlation times τ_s and τ_l of TEMPO in OTP. T_c is the MCT critical temperature. Continuous line: fit with DSE. Dotted line: guide for the eyes. Dashed line: fit with Arrhenius laws.

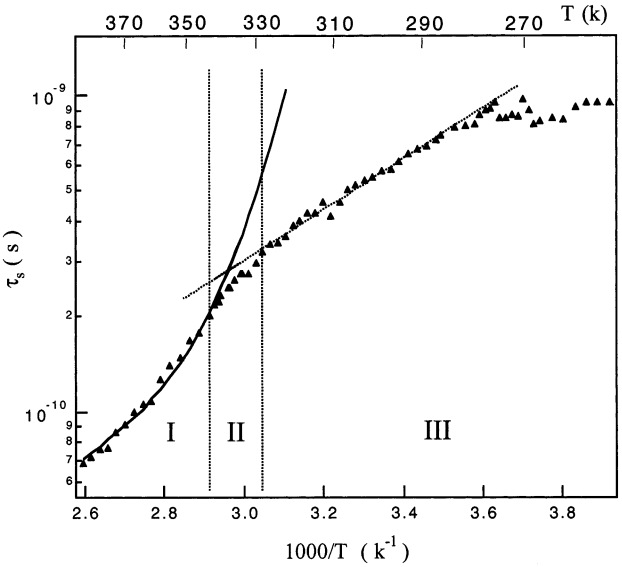

Figure 6. Temperature dependence of the short-time correlation time τ_s of CHOLESTANE in OTP. Continuous line: fit with DSE. Dotted line: fit with Arrhenius law. The activation energy and attempt rate are 15.0 $\pm$ 1.3 kJ/mol and 7.2 $\times 10^{11}$ s^{-1}, respectively.

The spinning correlation time at short time $\tau_{||s}$ of CHOLESTANE dissolved in OTP is presented in Figure 6. The anisotropy ratio does not exhibit appreciable changes in the overall temperature range we studied and $\tau_{\perp s}/\tau_{||s} = 5$.[39] Henceforth, $\tau_{||s}$ will be referred to as τ_s. The plot shows three different dynamical regions in close analogy to TEMPO. In region I ($T > T_{D-I} \equiv 342$ K), which extends over 40 K, τ_s is proportional to the viscosity. At 342 K, the reorientation decouples from the viscosity on the short-time scale and the crossover region II is entered. Region II extends over about 15 K down to 328 K and is shown in Figure 7 as a function of η/T. Below $T_{I-A} \equiv$ 328 K, activated reorientation is apparent with a knee at $T_{A-A} \equiv$ 281 K and CHOLESTANE reorientates on a short time scale in a frozen host. The crossover temperatures between the

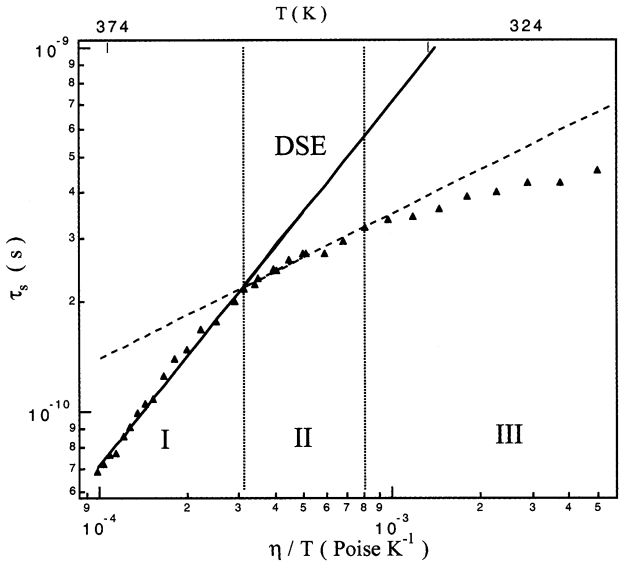

Figure 7. Region II of CHOLESTANE in OTP as a function of η/T. The continuous line is the prediction by DSE (see also Figure 6). The dashed line is a guide for the eyes. Note the change of dynamical regime occurring at the boundaries of the region at 342 and 328 K.

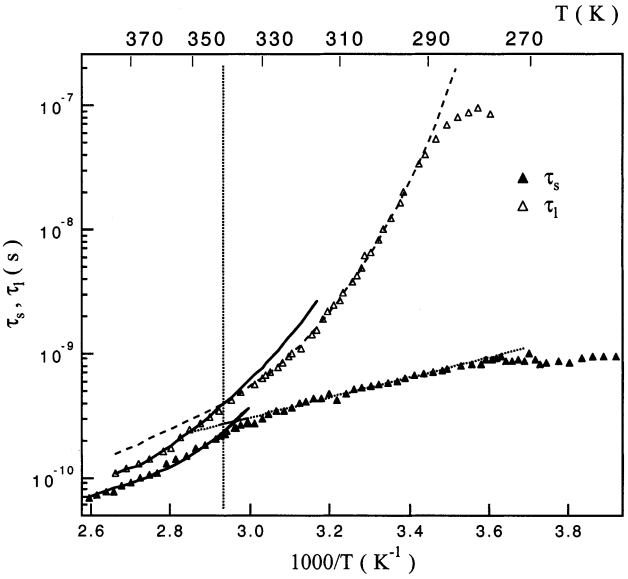

Figure 8. Comparison of the temperature dependence of the spinning correlation times τ_s and τ_l of CHOLESTANE in OTP. Continuous line: fit with DSE. Dashed line: guide for the eyes. Dotted line: fit with Arrhenius laws. The vertical line marks the temperature where the decoupling from the viscosity occurs at short (342 K) and long times (340 K).

dynamical regimes of the short-time reorientation of CHOLESTANE and other relevant quantities are summarized in Table 1.

Figure 8 shows the comparison between the spinning motion of CHOLESTANE at long and short time. A thorough discussion of the spinning and tumbling correlation times at long times of CHOLESTANE in OTP can be found in ref 7. Again, similarly to the TEMPO tracer, the long-time and the short-time dynamics exhibit close analogies. For $T > 340$ K, $\tau_s \approx \tau_l$ and the correlation loss is exponential (see section 2). τ_l is in quantitative agreement with the extension of DSE to the case of prolate ellipsoid.[7] The fit yields semiaxis $r_{||} = 11$ Å, $r_{\perp} = 2.6$ Å with slip boundary conditions to be compared to the van der Waals values $a_{||} \approx 9.9$ Å and $a_{\perp} \approx 2.9$ Å. At 340 K τ_l and the viscosity decouples. Remarkably, the reorientation at short

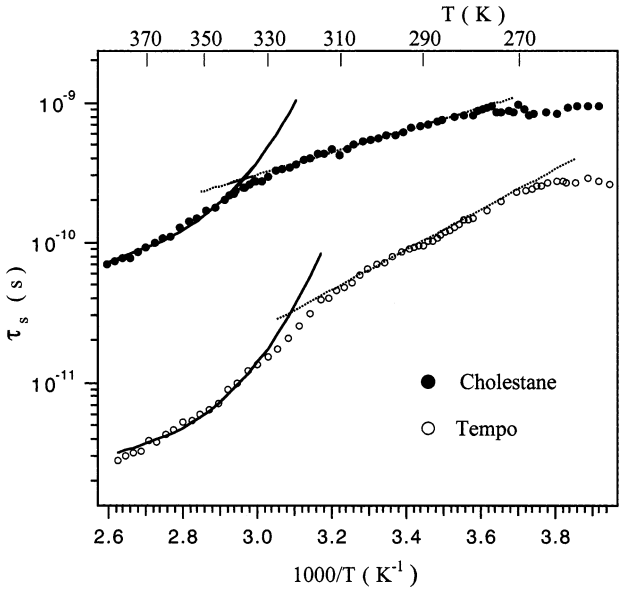

Figure 9. Comparison of the temperature dependence of the correlation times at short time τ_s for the TEMPO and CHOLESTANE tracers in OTP. Continuous line: fit with DSE. Dashed line: fit with Arrhenius laws.

time decouples from the viscosity at 342 K. For $T < 340$ K, τ_l increases according to FDSE over about two decades.[7] Around $T_c = 290$ K a knee in the temperature dependence of τ_l is apparent. Unfortunately, the ESR data may be collected only down to 278 K, where the spectroscopy reaches the powder limit and becomes insensitive to the reorientation of the tracer.[27−30] Interestingly, the knee on the long-time dynamics at T_c compares well with the knee at $T_{A-A} = 281$ K, which is observed in the short-time dynamics.

The rotational dynamics of our stiff tracers in supercooled and glassy OTP at short and long time shows a number of common features: a high-temperature region where DSE holds, an intermediate region, and an activated region at lower temperatures. Nonetheless, the temperatures at which the two tracers change dynamical regimes and the activation energies are different. From this respect the Arrhenius plots of the correlation times τ_s of both tracers are compared in Figure 9. We believe that these differences are not trivial consequences due to the use of different tracers but they may be reconciled on a different ground. To this aim, let us consider the following scaling of the rotational correlation times at *short* time:

$$\begin{cases} T \rightarrow T^* \equiv T/T_{rif} \\ \tau \rightarrow \tau^* \equiv A\tau^{1/\xi} \end{cases} \tag{5}$$

where T_{rif} is a reference temperature and A and ξ are constants. If T is in the range where DSE (eq 1) holds, the equality $\xi = 1$ is understood. Figure 10 shows that the rotational correlation times at short times of TEMPO and CHOLESTANE are collapsed by the above scaling in a single curve over a wide range of temperature, including both the intermediate region and the activated regime. Table 2 shows the virtual coincidence of the scaled crossover temperatures between the different rotational regimes at short times. Moreover, the table also lists the quantity $T_{A-A}\Delta E/\xi$, which, according to eq 5, should be constant. ξ is the slope of the dashed lines in Figures 4 and 7.

The above discussion leads to the conclusion that scaling by eq 5 removes the differences in the short-time reorientation, which may be ascribed to the different geometry and the specific solute−solvent interactions of the tracers. The scaling of the

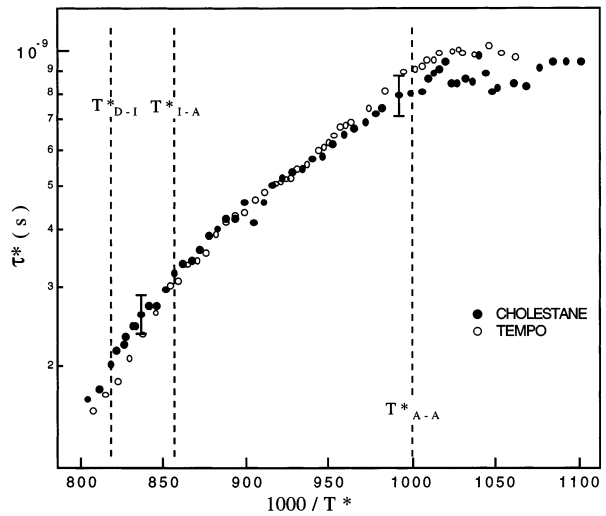

Figure 10. Scaling of the rotational correlation times at short times according to eq 5. $T_{rif} = T_{A-A}$ (see Table 1).

TABLE 2: Scaling of the Short-Time Reorientation of the Tracers[a]

tracer	T^*_{D-I}	T^*_{I-A}	ξ	$T_{A-A}\Delta E_1/\xi$	$T_{A-A}\Delta E_2/\xi$
TEMPO	1.23	1.17	0.57	12 800	1990
CHOLESTANE	1.22	1.17	0.37	11 400	1820

[a] Reduced crossover temperatures between the DSE and the intermediate regimes (T^*_{D-I}) and the intermediate- and the high-temperature activated regimes (T^*_{I-A}). The reduced temperature is defined as $T^* = T/T_{A-A}$. The inverse of the scaling exponent of eq 5, ξ, and the quantity $T_{A-A}\Delta E/\xi$ (in MKSA units) are also listed. For further details refer to Table 1.

short-time reorientation is demonstrated in a wide temperature range where, depending on the temperature, the tracers reorientate in a liquid, highly viscous, and solidlike host. Despite the quite different aspect ratios and sizes of the tracers, the reorientation of the two tracers may be scaled to a "universal" curve, suggesting that the tracers are accommodated in an environment with self-similar features. From this respect, it is worth noting that the scaling eq 5 does *not* hold at long times (τ_l) even if the tracers exhibit the usual three dynamical regimes.

Some final remarks are due to the crossover between the DSE (regions I) and the intermediate (regions II) regimes. At long times (τ_l) the crossover takes place at 298 K for TEMPO and 340 K for CHOLESTANE. At short times (τ_s) the crossover takes place at 333 K for TEMPO and 342 K for CHOLESTANE. In both cases, even if TEMPO reorientates faster than CHOLESTANE, the former decouples from η at lower temperatures than the latter and this effect is very pronounced at long times. The finding is by no means obvious and is at variance with the possibility that the decoupling between the rotational diffusion and the viscosity may be ascribed solely to some growing relaxation time scale of the host. In fact, in this case TEMPO should decouple at higher temperatures than CHOLESTANE.

5. Conclusions

The reorientation of stiff molecular tracers with very different aspect ratios and sizes in supercooled and glassy OTP has been investigated. The study has been carried out by linear (ESR) and nonlinear (LODESR) electron spin resonance spectroscopies.

The temperature dependences of the correlation times of the two tracers on the short (τ_s) and long (τ_l) time scale exhibit similar features. At higher temperatures, τ_l and τ_s are coupled to the shear viscosity of OTP according to DSE (liquid regime). With $\tau_s \cong \tau_l$, the rotational correlation loss is exponential. At intermediate temperatures the tracer reorientation decouples from the viscosity. At lower temperatures the host relaxation times exceed by many orders of magnitude the reorientation time of the tracer that rotates via activated jumps in a solidlike environment.[35] The transition region from one regime to another is quite narrow.

Despite the largely different aspect ratios and sizes, the temperature dependence of the correlation times at *short time* of the two tracers exhibits a scaling property (eq 5). The scaling, which is lost at long times, strongly relies on the fractional DSE analysis of the viscous regime since, the ξ exponent is explicitly used.[7] The rotational dynamics of the tracers in supercooled OTP suggests the existence of a characteristic length scale and then the presence of spatial heterogeneities.

References and Notes

(1) Einstein, A. *Investigations on The Theory of the Brownian motion*; Dover: New York, 1956.

(2) Debye, P. *Polar Molecules*; Dover: New York, 1929.

(3) Dale Favro, L. *Phys. Rev.* **1960**, *119*, 53. Hu, C. M.; Zwanzig, R. *J. Chem. Phys.* **1974**, *60*, 4354. Fleming, G. R.; Morris, J. M.; Robinson, G. W. *Chem. Phys.* **1976**, *17*, 91. Chuang, T. J.; Eisenthal, K. B. *J. Chem. Phys.* **1972**, *37*, 5094. Tao, T. *Biopolymers* **1969**, *8*, 609. Youngren, G. K.; Acrivos, A. *J. Chem. Phys.* **1983**, *79*, 3846.

(4) Rössler, E. *Phys. Rev. Lett.* **1990**, *65*, 1595.

(5) Rössler, E.; Tauchert, J.; Eiermann, P. *J. Phys. Chem.* **1994**, *98*, 8173.

(6) Cicerone, M. T.; Blackburn, F. R.; Ediger, M. D. *J. Chem. Phys.* **1996**, *104*, 7210.

(7) Andreozzi, L.; Di Schino, A.; Giordano, M.; Leporini, D. *Europhys. Lett.* **1997**, *38*, 669.

(8) Chang, I.; Fujara, F.; Geil, B.; Heuberger, G.; Mangel, T.; Sillescu, H. *J. Non-Cryst. Solids* **1994**, *172*, 248.

(9) Heuberger, G.; Sillescu, H. *J. Phys. Chem.* **1996**, *100*, 15255.

(10) Ehlich, D.; Sillescu, H. *Macromolecules* **1990**, *23*, 1600.

(11) Gold, D.; Onyenemezu, C.; Miller, W. *Macromolecules* **1996**, *29*, 5700.

(12) Andreozzi, L.; Di Schino, A.; Giordano, M.; Leporini, D. *Philos. Mag. B* **1998**, *77*, 547.

(13) Andreozzi, L.; Giordano, M.; Leporini, D. *J. Non-Cryst. Solids* **1998**, *235−237*, 219.

(14) Hall, D. B.; Dhinojwala, A.; Torkelson, J. M. *Phys. Rev. Lett.* **1997**, *79*, 103.

(15) Voronel, A.; Veliyulin, E.; Machavariani, V. Sh.; Kisliuk, A.; Quitmann, D. *Phys. Rev. Lett.* **1998**, *80*, 2630.

(16) Schmidt-Rohr, K.; Spiess, H. W. *Phys. Rev. Lett.* **1991**, *66*, 3020.

(17) Böhmer, R.; Hinze, G.; Diezemann, G.; Geil, B.; Sillescu, H. *Europhys. Lett.* **1996**, *36*, 55.

(18) Kob, W.; Donati, C.; Plimpton, S. J.; Poole, P. H.; Glotzer, S. C. *Phys. Rev. Lett.* **1997**, *79*, 2827.

(19) Donati, C.; Douglas, J. F.; Kob, W.; Plimpton, S. J.; Poole, P. H.; Glotzer, S. C. *Phys. Rev. Lett.* **1998**, *80*, 2338.

(20) Sillescu, H. *J. Non-Cryst. Solids* **1999**, *243*, 81.

(21) Hodgdon, J. A.; Stillinger, F. H. *Phys. Rev. E* **1993**, *48*, 207. Stillinger, F. H.; Hodgdon, J. A. *Ibid.* **1994**, *50*, 2064.

(22) Liu, C. Z.-W.; Oppenheim, I. *Phys. Rev. E* **1996**, *53*, 799.

(23) Leporini, D.; Douglas, J. F. *J. Non-Cryst. Solids* **1998**, *235−237*, 137.

(24) Nicodemi, M.; Coniglio, A. *Phys. Rev. E* **1998**, *56*, R39.

(25) Angelani, L.; Parisi, G.; Ruocco, G.; Viliani, G. *Phys. Rev. Lett.* **1998**, *81*, 4648.

(26) Yamamoto, R.; Onuki, A. *Phys. Rev. E*, in press (cond-mat/9806207).

(27) Muus, L. T., Atkins, P. W., Eds. *Electron Spin Relaxation in Liquids*; Plenum Press: New York, 1972.

(28) Berliner, L. J., Ed. *Spin Labeling Theory and Applications*; Academic: New York 1976; Academic Press: New York, 1979; Vols. 1 and 2.

(29) Andreozzi, L.; Giordano, M.; Leporini, D. In *Structure and Transport Properties in Organized Polymeric Materials*; Chiellini, E., Giordano, M., Leporini, D., Eds.; World Scientific: Singapore, 1997. Andreozzi, L.; Donati, C.; Giordano, M.; Leporini, D. *Ibid.*

(30) Slichter, C. P. *Principles of Magnetic Resonance*; Springer: Berlin, 1990. Gordy, W. *Theory and Applications of Magnetic Resonance*; Wiley: New York, 1980.

(31) Giordano, M.; Grigolini, P.; Leporini, D.; Marin, P. *Adv. Chem. Phys.* **1985** *62*, 321.

(32) Favro, D. L. *Phys. Rev.* **1960**, *119*, 53.

(33) Andreozzi, L.; Di Schino, A.; Giordano, M.; Leporini, D. *J. Phys.: Condens. Matter* **1996**, *8*, 9605.

(34) Valiev, K. A.; Ivanov, E. N. *Sov. Phys.-Usp.* **1974**, *16*, 1.

(35) Andreozzi, L.; Cianflone, F.; Donati, C.; Leporini, D. *J. Phys.: Condens. Matter* **1996**, *8*, 3795.

(36) Giordano, M.; Leporini, D.; Martinelli, M.; Pardi, L.; Santucci, S.; Umeton, C. *J. Chem. Phys.* **1988**, *88*, 607.

(37) Leporini, D. *Phys. Rev. A* **1994**, *49*, 992.

(38) Andreozzi, L.; Donati, C.; Giordano, M.; Leporini, D. *Phys. Rev. E* **1994**, *49*, 3488.

(39) Andreozzi, L. Ph.D. Thesis, Università di Pisa, 1997.

(40) According to the diffusion and the jump models, the rotational correlation functions are exponential. The derivation of eq 3 needs their power spectrum at ω_0, $J(\omega_0)$, which has the Debye form. In the slow-fluctuation regime, which is of main concern here, $J(\omega_0) \propto \omega_0^{-2}\tau_s^{-1}$. In supercooled liquids the distribution of correlation times is highly expected.[16−20] In this case $1/\tau_s$ must be read as $\langle 1/\tau_s \rangle$, where the brackets denote the average over the distribution.

(41) Cukiermann, M.; Lane, J. W.; Uhlmann, D. R. *J. Chem. Phys.* **1973**, *59*, 3639. Laughlin, W. T.; Uhlmann, D. R. *J. Phys. Chem.* **1972**, *76*, 2317.

(42) Götze, W.; Sjögren, L. *Rep. Prog. Phys.* **1992**, *55*, 241.